

# Isospin transport in $^{84}\text{Kr} + ^{112,124}\text{Sn}$ collisions at Fermi energies

S. Barlini,<sup>1,2</sup> S. Piantelli,<sup>1</sup> G. Casini,<sup>1</sup> P.R. Maurenzig,<sup>1,2</sup> A. Olmi,<sup>1,\*</sup> M. Bini,<sup>1,2</sup> S. Carboni,<sup>1,2</sup> G. Pasquali,<sup>1,2</sup> G. Poggi,<sup>1,2</sup> A.A. Stefanini,<sup>1,2</sup> R. Bougault,<sup>3</sup> E. Bonnet,<sup>4</sup> B. Borderie,<sup>5</sup> A. Chbihi,<sup>4</sup> J.D. Frankland,<sup>4</sup> D. Gruyer,<sup>4</sup> O. Lopez,<sup>3</sup> N. Le Neindre,<sup>3</sup> M. Pârlog,<sup>3,6</sup> M.F. Rivet,<sup>5</sup> E. Vient,<sup>3</sup> E. Rosato,<sup>7</sup> G. Spadaccini,<sup>7</sup> M. Vigilante,<sup>7</sup> M. Bruno,<sup>8</sup> T. Marchi,<sup>9</sup> L. Morelli,<sup>8</sup> M. Cinausero,<sup>9</sup> M. Degerlier,<sup>9</sup> F. Gramegna,<sup>9</sup> T. Kozik,<sup>10</sup> T. Twaróg,<sup>10</sup> R. Alba,<sup>11</sup> C. Maiolino,<sup>11</sup> and D. Santonocito<sup>11</sup>

(FAZIA Collaboration)

<sup>1</sup>*Sezione INFN di Firenze, Via G. Sansone 1, I-50019 Sesto Fiorentino, Italy*

<sup>2</sup>*Dipartimento di Fisica, Univ. di Firenze, Via G. Sansone 1, I-50019 Sesto Fiorentino, Italy*

<sup>3</sup>*LPC, IN2P3-CNRS, ENSICAEN et Université de Caen, F-14050 Caen-Cedex, France*

<sup>4</sup>*GANIL, CEA/DSM-CNRS/IN2P3, B.P. 5027, F-14076 Caen cedex, France*

<sup>5</sup>*Institut de Physique Nucléaire, CNRS/IN2P3, Université Paris-Sud 11, F-91140 Orsay cedex, France*

<sup>6</sup>*Horia Hulubei, National Institute of Physics and Nuclear Engineering, RO-077125 Bucharest-Măgurele, Romania*

<sup>7</sup>*Dipartimento di Scienze Fisiche e Sezione INFN,*

*Università di Napoli “Federico II”, I 80126 Napoli, Italy*

<sup>8</sup>*INFN e Università di Bologna, 40126 Bologna, Italy*

<sup>9</sup>*INFN LNL Legnaro, viale dell’Università 2, 35020 Legnaro (Padova) Italy*

<sup>10</sup>*Jagiellonian University, Institute of Nuclear Physics IFJ-PAN, PL-31342 Kraków, Poland*

<sup>11</sup>*INFN LNS, via S.Sofia 62, 95125 Catania, Italy*

(Dated: June 18, 2018)

Isotopically resolved fragments with  $Z \lesssim 20$  have been studied with high resolution telescopes in a test run for the FAZIA collaboration. The fragments were produced by the collision of a  $^{84}\text{Kr}$  beam at 35 MeV/nucleon with a n-rich ( $^{124}\text{Sn}$ ) and a n-poor ( $^{112}\text{Sn}$ ) target. The fragments, detected close to the grazing angle, are mainly emitted from the phase-space region of the projectile. The fragment isotopic content clearly depends on the n-richness of the target and it is a direct evidence of isospin diffusion between projectile and target. The observed enhanced neutron richness of light fragments emitted from the phase-space region close to the center of mass of the system can be interpreted as an effect of isospin drift in the diluted neck region.

PACS numbers: 25.70.Lm, 25.70.Mn

## I. INTRODUCTION

The production of many fragments with different sizes is one of the main features of heavy-ion reactions at bombarding energies higher than 15-20 MeV/u. The mechanisms governing their production have been extensively investigated in the past. When the primary fragments produced in the interaction are sufficiently excited, their detection occurs after a de-excitation phase that may strongly alter their original identity. Various de-excitation processes are indeed possible and they depend both on the initial conditions and on the internal structure of the nuclei involved in the de-excitation path.

In recent years many experimental and theoretical (see [1–5] and references therein) efforts have been devoted to the investigation of the neutron-to-proton ratio  $N/Z$  (often called isospin) degree of freedom and to unravelling its influence on the reaction dynamics and on the subsequent decay processes. This was obtained either by using reaction partners with different isospin content or by comparing data from reactions involving different isotopic combinations of the projectile and/or of the target

[6–14]. From an experimental point of view, this kind of investigation requires detectors capable of good isotopic identification of the reaction products on an extended  $Z$  range.

The study of the isospin content of the emitted fragments and light particles, possibly complemented by a characterization of their emitting source [14–16], gives clues on different processes of isospin transport. One, called isospin “diffusion”, is related to the isospin asymmetry of a system in which projectile and target have different  $N/Z$  values [4–6, 10–12, 17–19]; the other, called isospin “drift” (or “migration”), is related to the density gradient which is expected to exist in the “neck” region, even between two identical nuclei [3, 16, 17, 20–22]. In both cases the experimental observables associated with the isospin content of the reaction products can be used to extract information on the symmetry energy term of the nuclear equation of state, via comparison with theoretical models [1, 3–5, 9–11, 14, 17–19, 23–27].

Many experiments found evidences of isospin transport in dissipative collisions at Fermi energies [2, 10–15, 19, 20]. In this paper we show some results obtained by bombarding with a  $^{84}\text{Kr}$  beam at 35 MeV/u two targets with different isospin:  $^{112}\text{Sn}$  and  $^{124}\text{Sn}$ . In the following we will often use “n-poor” and “n-rich system” to refer to the collision of the Kr beam with these

\*corresponding author; e-mail:olmi@fi.infn.it

two different targets. Although the light complex fragments detected in our experiment originate mainly from the quasi-projectile source, their isospin content shows a clear dependence on the target isotope.

## II. THE EXPERIMENT

The data presented in this paper have been collected by the FAZIA collaboration [28] at the Superconducting Cyclotron of the Laboratori Nazionali del Sud (LNS) of INFN, in Catania, during a recent test experiment [29]. A pulsed beam ( $\delta t \approx 1$  ns FWHM) of  $^{84}\text{Kr}$  at 35 MeV/nucleon impinged on isotopically enriched targets of  $^{112}\text{Sn}$  ( $415 \mu\text{g}/\text{cm}^2$ ) and  $^{124}\text{Sn}$  ( $600 \mu\text{g}/\text{cm}^2$ ). The  $N/Z$  of the beam was 1.33, intermediate between that of the two targets of  $^{112}\text{Sn}$  ( $N/Z=1.24$ ) and  $^{124}\text{Sn}$  ( $N/Z=1.48$ ). In the past these systems (and other similar Kr or Sn induced reactions, in direct or reverse kinematics) have been the subject of extensive investigations at comparable bombarding energies by other groups [9–15, 19, 24], so that they represent a good benchmark for a test experiment.

Here we analyze the data of a three-element telescope (Si1-Si2-CsI(Tl)) located at an angle of  $5.4^\circ$  and at 100 cm distance from the target. The silicon detectors (manufactured by FBK [30]) were ion-implanted of the neutron transmutation doped (n-TD) type, with bulk resistivity values in the range 3000–4000  $\Omega\text{cm}$  and good doping uniformity (of the order of 3% FWHM [31]). The silicon layers were obtained from “random” cut wafers (about  $7^\circ$  off the  $\langle 100 \rangle$  axis) to minimize channeling effects [32]. They were in transmission mounting, with dead layers on both sides of  $\sim 500$ – $800$  nm and had an active area of  $20 \times 20 \text{ mm}^2$ . The thickness of Si1 and Si2 was  $305 \mu\text{m}$  and  $510 \mu\text{m}$ , respectively, with a measured non-uniformity of the order of  $1 \mu\text{m}$ . The CsI(Tl) crystal (manufactured by Amcryst [33]) was 10 cm thick, with an excellent doping uniformity (of the order of 5%), and it was read out by a photodiode. The telescope was equipped with custom-built high-quality electronics. More details on the characteristics of the setup and on the obtained performances are given elsewhere [29, 31, 32, 34–37]. Here we briefly remind that the charge and current signals produced in low-noise preamplifiers [38], mounted in vacuum next to the detectors, are sampled by fast digital boards purposely built by the FAZIA group. For each detector, the sampled signals are then stored for off-line analysis. Energy information from the two silicon detectors was obtained by means of trapezoidal shaping of the digitized signals (see [35] for details). For energy calibration, the so-called “punch-through energies” [39] of light identified ions were used, as described also in [35].

In this work we concentrate on identified fragments ( $Z \geq 3$ ) that are stopped in the second silicon layer or in the CsI(Tl). The kinetic energy of fragments stopped in Si2 is the sum of the two silicon energies  $E_{\text{sum}} = E_1 + E_2$ .

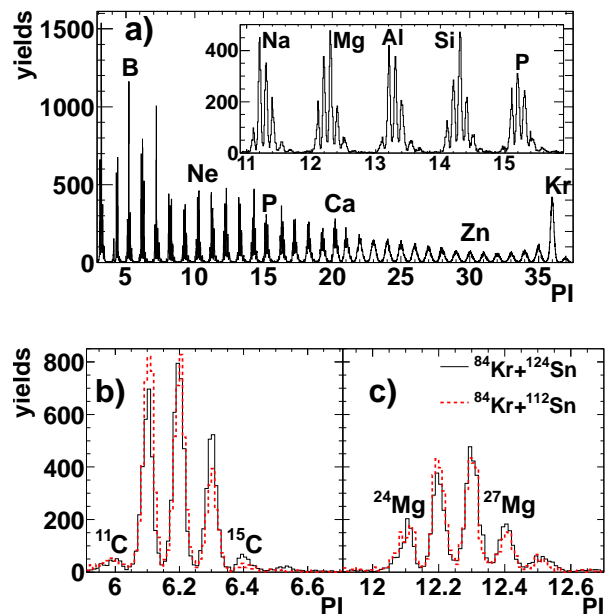


FIG. 1: (Color online) (a) Particle Identification (PI) spectrum for fragments passing the first silicon detector and stopped in the second one or in the CsI(Tl) crystal, for the reaction  $^{84}\text{Kr} + ^{124}\text{Sn}$ ; the inset is an expansion of the region  $Z=11$ – $15$ . (b) PI spectra for Carbon isotopes in the reactions  $^{84}\text{Kr} + ^{124}\text{Sn}$  (black histogram) and  $^{84}\text{Kr} + ^{112}\text{Sn}$  (dashed red); the spectra are normalized to the same total number of counts of C. (c) Same as (b), but for Mg isotopes.

When reaching the CsI(Tl) crystal, the full kinetic energy  $E$  is estimated from  $E_{\text{sum}}$  (which is now the energy-loss over the known total thickness of the two silicon detectors) with the help of range-energy tables [40–42], whose proper use requires the knowledge of  $Z$  and  $A$  of the ion.

The particle identification is given by the ridges in the correlations  $E_1$ – $E_2$  between the energies of the two silicon layers, or  $E_{\text{sum}}$ –LO between the silicon energy and the Light-Output of the CsI(Tl). The linearization of the ridges gives the so-called Particle Identification (PI). The high quality of the detectors and of the dedicated electronics allows isotopic resolution up to  $Z \approx 20$  (close to the limit reported in [35]), as shown in Fig. 1(a) by the PI spectrum for the n-rich target (the inset is a zoom of the region between  $Z=11$  and  $Z=16$ ). Figures 1(b) and (c) are the PI spectra for C and Mg isotopes, respectively. The black solid histograms correspond to the n-rich target and the red dashed ones to the n-poor target. For each element, the two histograms are normalized to the same number of counts. One sees at first glance that the isotopic composition is different in the two reactions. For each element, mass values are assigned to the PI peaks by comparing the isotopic ridges in the already mentioned correlations with the theoretical lines calculated from energy-loss tables.

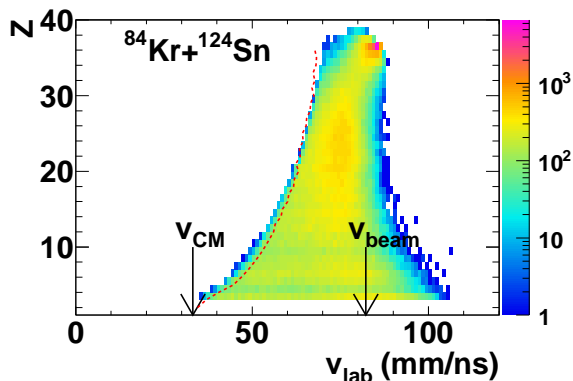


FIG. 2: (Color online) Charge vs. laboratory-velocity for  $Z \geq 3$  fragments passing the first silicon detector in the reaction  $^{84}\text{Kr} + ^{124}\text{Sn}$ . Arrows indicate the center-of-mass and beam velocities. The red dashed line is the expected threshold due to the first silicon detector.

### III. RESULTS

The telescope spanned the angular range from about  $4.8^\circ$  to  $6^\circ$ , just beyond the grazing angles of the two reactions (estimated to be about  $4.1^\circ$  and  $4.0^\circ$  for the n-poor and n-rich system, respectively), therefore its position was well suited for a good sampling of a large variety of fragments, mainly originating from the quasi-projectile (QP) phase-space. We want to stress that the beam and the setup are the same, the kinematics is very similar and the only relevant difference between the two systems is the neutron number of the target nucleus. Since we are mainly dealing with fragments originating from the QP phase-space, any substantial difference between the two sets of data has to be attributed to a transport of isospin between projectile and target.

From the large number of experiments performed in many years of investigation of heavy-ion collisions in the Fermi energy regime, we now know that: a) we mainly deal with binary dissipative collisions producing excited quasi-projectiles (QP) and quasi-targets (QT); b) their decay is dominated by evaporation, in competition with fission-like processes, especially for massive nuclei or large excitations; c) the most central collisions involve fusion-like phenomena, with the formation of a big transient system, which may then undergo a multifragmentation decay; d) non-equilibrium phenomena are present, consisting in the rapid emission of light reaction products (neck emissions [44, 45]), or in the occurrence of fission-like processes retaining some memory of the preceding dynamics (fast oriented fission [15, 46–48]).

The origin of the detected reaction products is often deduced from the correlation charge vs. laboratory velocity (see, e.g., [2, 15, 49, 50]). An example is shown in Fig. 2 for the reaction  $^{84}\text{Kr} + ^{124}\text{Sn}$  (a similar plot is obtained also for  $^{84}\text{Kr} + ^{112}\text{Sn}$ ). The laboratory velocity is deduced from the measured energy, using the identified mass (up

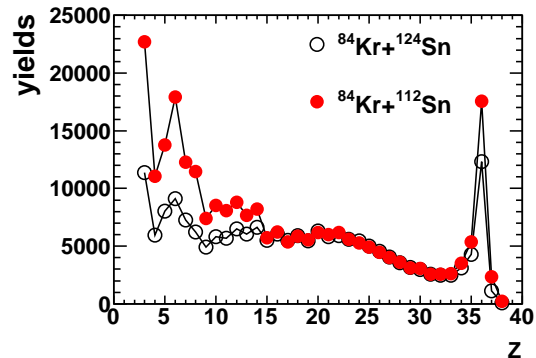


FIG. 3: (Color online) Inclusive charge distribution of fragments ( $Z \geq 3$ ) produced in the reactions of  $^{84}\text{Kr}$  on  $^{124}\text{Sn}$  (black open dots) and  $^{112}\text{Sn}$  (red solid dots) at 35 MeV/u. The distributions are normalized in the region  $18 \leq Z \leq 28$  (see text).

to  $Z \sim 20$ ) or the mass estimated from the Evaporation Attractor Line (EAL) [43] for heavier elements.

The dashed line indicates the estimated  $Z$ -dependent threshold due to the requirement of passing through the first silicon detector. The arrows, corresponding to the velocities of the center of mass and of the beam (33.2 and 82.2 mm/ns, respectively), indicate that practically all measured fragments are forward-emitted in the center-of-mass system and that the velocities of the heavier ones are not too different from that of the projectile. Therefore one can infer that the fragments originate indeed from the QP, with almost no contamination from the QT (in the analysis we reject very light fragments with  $v_{\text{lab}} < 40$  mm/ns), and that there could be -at most- some contribution from the “neck region” (i.e. the phase space region corresponding to the contact zone of the colliding nuclei).

From the quasi-elastic peak (near  $Z=36$  and  $v=82.2$  mm/ns), an evident ridge (only marginally affected by the threshold) develops towards lower velocities and lighter fragments. This is a characteristic feature of binary dissipative collisions [15, 51]: with decreasing velocity, the QP excitation increases, so that it is detected as a lighter QP remnant [20, 52] after a long decay chain. Indeed statistical calculations with the code GEMINI [53] show that an excited  $^{84}\text{Kr}$  nucleus, with a typical excitation energy of 300 MeV and spin  $30 \hbar$ , ends up in a bell-shaped distribution centered at  $Z \sim 28$ , with a tail extending down to  $Z \sim 20$ . Of course, because of possibly early dynamical emissions, the evaporating QP can be somewhat lighter than the projectile; as an example, in  $^{64}\text{Zn} + ^{64}\text{Zn}$  at 45 MeV/nucleon [20] the reconstructed primary QP charges were  $\sim 20\%$  smaller than  $Z=30$ , already for moderate dissipations. In Fig. 2 the most probable velocity of the ridge saturates at  $\sim 75$  mm/ns in correspondence with the broad charge distribution visible around  $Z=15-25$ . Assuming a binary kinematics, as it

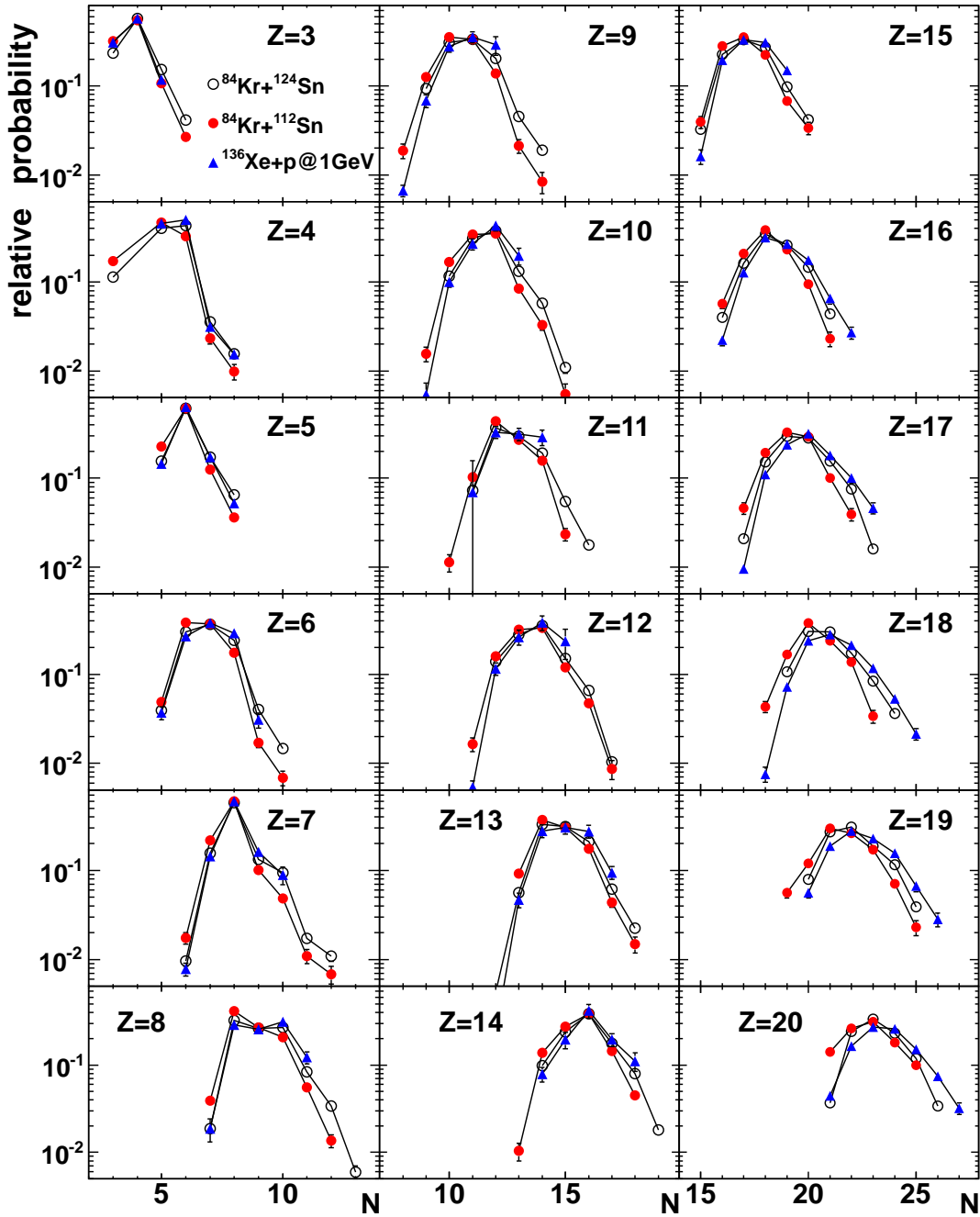


FIG. 4: (Color online) Relative probability of isotopic population for elements with  $Z=3$ – $20$ , obtained by normalizing each isotopic distribution to unity. The data are from the reactions  $^{84}\text{Kr}+^{124}\text{Sn}$  (open black dots) and  $^{84}\text{Kr}+^{112}\text{Sn}$  (solid red dots) at 35 MeV/u, and from  $^{136}\text{Xe}+\text{H}$  (blue triangles) at 1 GeV/u [54]. Bars represent statistical errors.

was done in [9], one would estimate a dissipation of about 500 MeV and an average excitation energy per nucleon of about 2.4 MeV. Here one can expect a sizable contribution from excited QPs undergoing a fission-like breakup, with a wide range of charge asymmetries. Finally, in the region of intermediate mass fragments (IMF, with  $3 \leq Z \lesssim 16$ ), the velocity distribution spreads out, spanning a wider range (especially towards lower velocities, where

it is more influenced by the detection threshold), while the most probable velocity value shows a weak increasing trend. This region is likely populated by the already mentioned neck emissions or by very asymmetric, possibly non-equilibrated, fission-like processes [15, 46–48]).

Further insight into the reaction processes can be gained by looking at the inclusive charge distributions of Fig. 3, which have been normalized in the range



$18 \leq Z \leq 28$ , where a fragment is either a QP remnant or the heavier fragment of a binary split of the QP (quasi-elastic fragments with  $Z \geq 29$  are not used because their yield is too sensitive to the small difference in grazing angle between the two reactions or to an exact alignment of the beam). This normalization roughly corresponds to considering the same number of inelastic binary or quasi-binary events. The comparison of the two distributions clearly shows that the n-poor system  $^{84}\text{Kr} + ^{112}\text{Sn}$  produces appreciably more IMFs. This is probably due to the fact that in the n-poor system the break-up into lighter fragments with  $Z < 15$ , either by fission or fragmentation, is favored with respect to the n-rich system.

The good isotopic resolution of the telescope allows to investigate the isotopic composition of the fragments. For each element from  $Z=3$  to  $Z=20$ , Fig. 4 shows the relative probability of observing the various isotopes in the collision of  $^{84}\text{Kr}$  with  $^{112}\text{Sn}$  (red full dots) and  $^{124}\text{Sn}$  (black open dots). Similarly to the C and Mg isotopes of Fig. 1(b) and (c), one finds –for all fragments and not only for the lighter ones– that the n-rich side is more populated for  $^{124}\text{Sn}$  than for  $^{112}\text{Sn}$  and, vice-versa, the n-poor side is more populated for  $^{112}\text{Sn}$  than for  $^{124}\text{Sn}$ .

A more quantitative estimate of the different contributions of the two reactions to the n-rich and n-poor sides of the isotope distributions of Fig. 4 is given by the average number of neutrons per charge unit  $\langle N \rangle / Z$ . This is an isospin sensitive variable which has been often used in the literature. Values of  $\langle N \rangle / Z$  are shown in Fig. 5(a) as a function of  $Z$  for the two collisions studied in this paper. In the n-rich system this ratio is systematically higher than in the n-poor one, by an amount of about 0.03–0.05. Since the largest part of the observed fragments belongs to the QP region of the phase-space (see Fig. 2), the observed difference clearly demonstrates the action of an isospin diffusion mechanism: the different isospin of the detected fragments depends on the n-richness of the target with which the projectile has interacted.

We can compare our results with published isotope-resolved cross sections (from mass spectrometer measurements at high bombarding energies), although some caution is required due to our thresholds (see Fig. 2). The blue triangles of Fig. 4 refer to published data [54] for the spallation of 1 GeV/u  $^{136}\text{Xe}$  nuclei impinging on an Hydrogen target. The data of [54] are not very different from the results of this paper: the main difference is that the abundance of isotopes on the n-rich side of the distribution is further increased with respect to our  $^{124}\text{Sn}$  (by an amount of the order of the difference between our two systems), and the abundance of isotopes on the n-poor side is further depressed with respect to our  $^{112}\text{Sn}$  (by about the same quantity). The similarity with our results is quite surprising if one considers two facts: first, spallation is a reaction mechanism completely different from that of our collisions and, second, the isospin of  $^{136}\text{Xe}$  ( $N/Z=1.52$ ) is considerably larger not only than the  $^{84}\text{Kr}$  beam (1.33), but also than the equilibrium value (1.42) of our system. These observations suggest that the

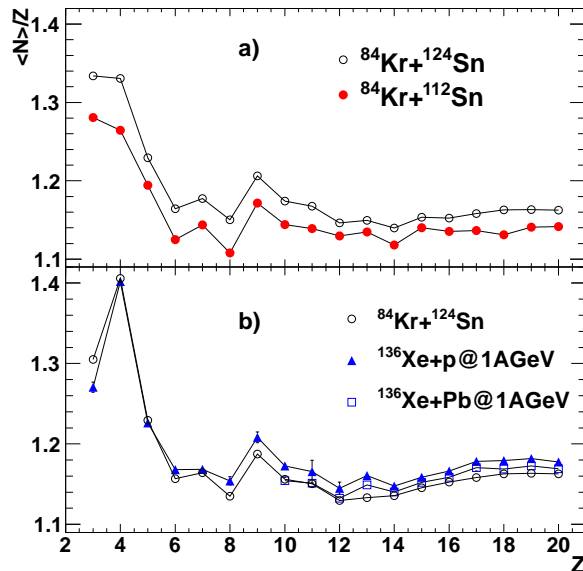


FIG. 5: (Color online) (a)  $\langle N \rangle / Z$  as a function of  $Z$  for the reaction  $^{84}\text{Kr} + ^{124}\text{Sn}$  (black open dots) and  $^{84}\text{Kr} + ^{112}\text{Sn}$  (red full dots) at 35 MeV/u. Statistical errors are smaller than dot size. (b) Comparison of  $\langle N \rangle / Z$  for 35 MeV/u  $^{84}\text{Kr} + ^{124}\text{Sn}$ , (black open dots), 1 GeV/u  $^{136}\text{Xe} + \text{H}$  (blue triangles [54]) and 1 GeV/u  $^{136}\text{Xe} + \text{Pb}$  (open squares [55]), computed in the same common range of isotopes.

final fragment isospin content bears little dependence in the preceding dynamics, but it retains memory of the original neutron richness.

In Fig. 5(b), the isospin sensitive variable  $\langle N \rangle / Z$  deduced from our n-rich system  $^{84}\text{Kr} + ^{124}\text{Sn}$  (black open dots) is compared with that from the  $^{136}\text{Xe}$  spallation (blue triangles, [54]) and the  $^{136}\text{Xe} + \text{Pb}$  collision (open squares, [55]; data available only for  $Z \geq 10$ ) at 1 GeV/u. Because of incomplete isotopic distributions in some set of data (see, e.g., the lack of  $^7\text{Be}$  and of n-rich isotopes with  $Z=7-12$  for the data of [54] in Fig. 4), a more meaningful comparison is obtained in Fig. 5(b) by computing  $\langle N \rangle / Z$  only from the isotopes that are common to the various sets of data. Remarkably the lightest fragments of [54] display a behavior very similar to that of our data. Above  $Z \approx 8$ , the only significant difference is that the fragments from the high-energy  $^{136}\text{Xe}$  reactions present just slightly higher values of  $\langle N \rangle / Z$  with respect to the  $^{84}\text{Kr} + ^{124}\text{Sn}$  reaction. Similar differences with target isospin have been observed in the reactions  $^{84}\text{Kr} + ^{92,98}\text{Mo}$  at 22 MeV/u [56]. However, those data are not included in Fig. 5(b), because it is not specified which isotopes were detected. On the contrary, in the reactions  $^{86}\text{Kr} + ^{27}\text{Al}$ ,  $^{103}\text{Rh}$ ,  $^{197}\text{Au}$  at 44 MeV/u, apparently no clear target dependence was observed [57].

One may wonder whether there is a difference in the isospin content of the fragments produced in the

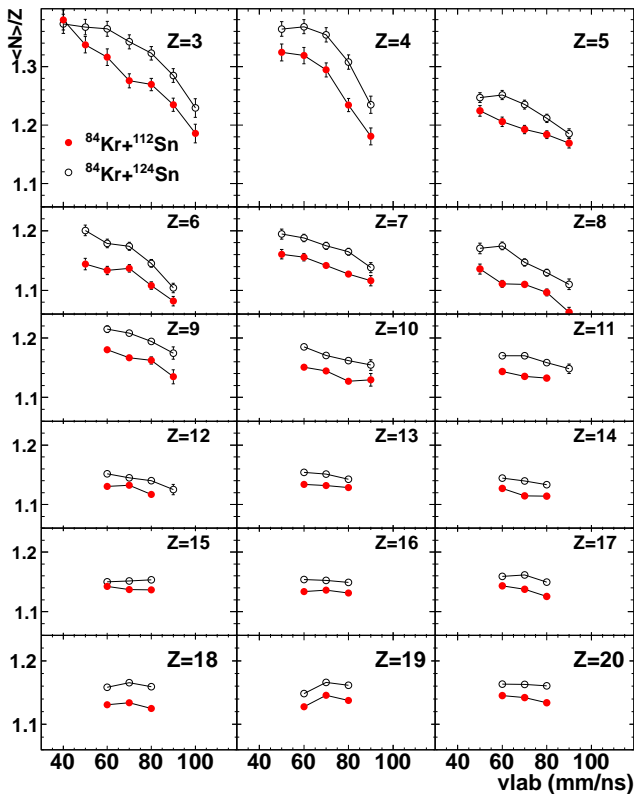


FIG. 6: (Color online)  $\langle N \rangle / Z$  as a function of the laboratory velocity for the reaction  $^{84}\text{Kr}+^{124}\text{Sn}$  (black points) and  $^{84}\text{Kr}+^{112}\text{Sn}$  (red points). Each panel refers to a different element from  $Z = 3$  to  $Z = 20$ . Error bars combine statistical errors and uncertainties in the isotope identification.

$^{84}\text{Kr}+^{124}\text{Sn}$  and  $^{84}\text{Kr}+^{112}\text{Sn}$  reactions, depending on the phase-space region they belong to. For this purpose, Fig. 6 shows the evolution of  $\langle N \rangle / Z$  for each element (from  $Z = 3$  up to  $Z = 20$ ) as a function of the laboratory velocity of the fragments. The most evident effect is that, again, the black open dots (n-rich system) are always above the red full dots (n-poor system). This is an effect of the isospin diffusion, due to the interaction of the projectile with targets of different isospin content. The second clear observation is that for light ions  $\langle N \rangle / Z$  rapidly decreases with increasing velocity, while it displays a rather flat behavior for heavier ions. The third point worth noting is that the highest values of  $\langle N \rangle / Z$  of fragments with  $Z=3-4$  are reached at the smallest laboratory velocities (close to that of the center of mass).

Given the experiment geometry ( $4.8^\circ \leq \theta_{\text{lab}} \leq 6^\circ$ ), the fragments with large velocities (of the order of that of the beam) are likely to be emitted in forward direction from an excited QP, while those with lower velocities are expected to be emitted by the same QP in backward direction, with possible contributions from midvelocity- (or neck-) emissions. In fact, at Fermi energies, fragments may be produced not only by a fission-like equilibrated decay of the QP (or QT), but also by the breakup of

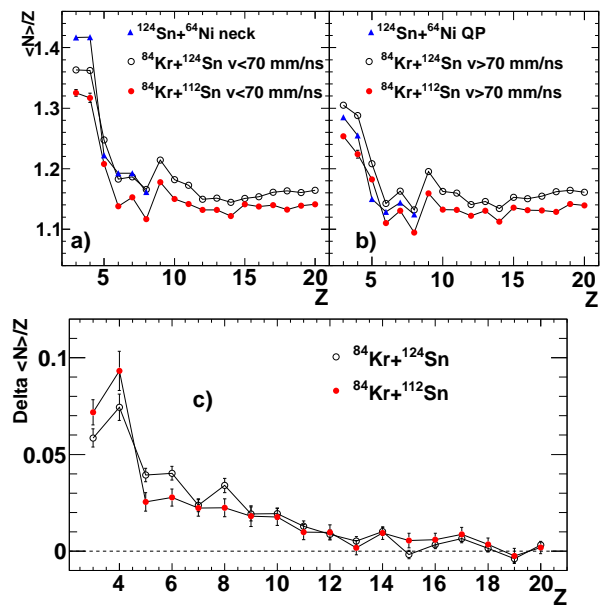


FIG. 7: (Color online)  $\langle N \rangle / Z$  as a function of  $Z$  in the n-rich (open black dots) and n-poor system (full red dots), for (a)  $v_{\text{lab}} < 70$  mm/ns and (b)  $v_{\text{lab}} \geq 70$  mm/ns. Blue triangles: results of reference [14]. (c) Differences between backward and forward values of  $\langle N \rangle / Z$  for the two reactions of this paper.

an elongated neck-like structure [58] formed between QP and QT. It has been shown [59] that these fragments present a kind of “hierarchy effect”: lighter fragments originating from the thinner central part of the rupturing neck have small velocities in the center of mass frame, while heavier fragments produced in thicker zones of the neck possess larger velocities, close to (but still smaller than) that of the QP (or QT). Therefore, in this picture the low-velocity lightest fragments ( $Z=3, 4$  and partially 5) of Fig. 6 are probing the most central part of the neck and thus their higher values of  $\langle N \rangle / Z$  could be an indication of isospin drift, namely a neutron enrichment of the more diluted central region of the neck [17]. On the contrary, heavier fragments with  $Z \gtrsim 12$  have a low  $\langle N \rangle / Z$  (around 1.15) with practically no dependence on the emission velocities, which however span a rather narrow range of about 20-30 mm/ns around  $v_{\text{lab}} \approx 70$  mm/ns.

It is interesting to compare the data of Fig. 6 with the results [14] of the similar system  $^{124}\text{Sn}+^{64}\text{Ni}$  at 35 MeV/u. In [14] the assumed neck emissions and the more equilibrated decays of the QP have been selected on the basis of an angular correlation of the observed fragments. In our case, since we have only a single detected fragment, the selection is made on the basis of the laboratory velocity. In figure 7, the ratio  $\langle N \rangle / Z$  as a function of  $Z$  is presented for  $v_{\text{lab}} < 70$  mm/ns (a) and  $v_{\text{lab}} \geq 70$  mm/ns (b) for the two systems measured in this work (open black and full red dots for the n-rich

and n-poor system, respectively). These two selections on  $v_{\text{lab}}$  roughly correspond to light fragments emitted in backward and forward direction in the frame of a QP. The blue triangles (available only for  $3 \leq Z \leq 8$ ) are the data of [14], ascribed (a) to neck emissions or (b) to QP emissions. Although the selections are not exactly the same, the remarkable agreement with our data supports the interpretation that low-velocity light fragments are emitted from the neck.

One may further note that, in both systems, our data show no appreciable forward-backward effect for fragments above  $Z \approx 10$ . This is better seen from Fig. 7(c), which shows the difference  $(\langle N \rangle / Z)_{\text{backw}} - (\langle N \rangle / Z)_{\text{forw}}$  for the n-rich and n-poor systems. Here the effects of the isospin diffusion mechanism, which in each system affects in the same way the forward- and backward-emitted isotopes, cancel out. Thus the positive signal that is apparent for the light fragments has to be considered a signature of isospin drift.

#### IV. SUMMARY AND CONCLUSIONS

We have presented data collected by the FAZIA collaboration during a test experiment with a setup of small solid angle, but of high quality performances in terms of isotopic resolution (up to  $Z=20$ ) for the systems  $^{84}\text{Kr}+^{112}\text{Sn}$  and  $^{84}\text{Kr}+^{124}\text{Sn}$  at 35 MeV/u.

The angular geometry of the setup (located close to the grazing angles for both reactions) allows to detect products originating from the quasi-projectile decay (including the quasi-projectile residue itself) and also from a phase-space region (close to the center of mass of the system) where a sizable contribution of light ions produced in the neck-zone is expected.

Even with this simple setup, one can obtain significant information on isospin transport processes. For each element, the relative yields show an enhancement of n-rich isotopes for the interaction of the  $^{84}\text{Kr}$  with a  $^{124}\text{Sn}$  target, and vice-versa an enhancement of n-poor isotopes for the interaction with a  $^{112}\text{Sn}$  target. The fact that fragments emitted from the QP display a different neutron enrichment depending on the different isospin content of the targets is a direct evidence of an isospin diffusion effect, i.e. the transport of nucleons between projectile and target with different  $N/Z$  during the interaction phase. The relative yields are quite similar to those obtained in [54] for the spallation of  $^{136}\text{Xe}$ , i.e. in a completely different scenario from the point of view of the reaction mech-

anism. The data show no appreciable dependence on the dynamics of the reaction. A signature of the previous history remains only in the differences in neutron richness associated with the different targets and the same  $^{84}\text{Kr}$  beam.

According to theoretical studies, the neck region should be diluted with respect to the normal nuclear density. On these grounds, an isospin drift is expected, which tends to increase the neutron richness of the neck region. This prediction appears to be confirmed by the present data. Light fragments, emitted in a possibly diluted phase-space region close to the center of mass of the system, display indeed a higher  $\langle N \rangle / Z$ , which strongly decreases when moving away from the neck region, towards the larger velocities typical of the decays of an excited QP.

On the contrary, heavier fragments (with  $Z \gtrsim 12$ ) do not show any dependence of their  $\langle N \rangle / Z$  on the velocity bin; this fact can be understood by assuming that heavier fragments originate from the quasi-projectile fission, i.e. they have all a common origin, independently of their laboratory velocity (which spans a considerably smaller range with respect to light fragments). The  $\langle N \rangle / Z$  associated to the n-poor system is always smaller than that associated to the n-rich system for all velocity bins.

The investigation of isospin transport needs further experiments and it will certainly benefit from the new facilities for radioactive beams now under construction and from large area multidetectors with A and Z identification, like FAZIA. In fact these phenomena will be strongly enhanced if the difference of isospin content between the interacting nuclei can be further increased.

#### Acknowledgments

The authors would like to thank the crew of the Superconducting Cyclotron, in particular D. Rifuggiato, for providing a very good quality beam, and the staff of LNS for continuous support. The support of the detector and mechanical workshops of the Physics Department of Florence is also gratefully acknowledged. The research leading to these results has received funding from the European Union Seventh Framework Programme FP7(2007-2013) under Grant Agreement No. 262010-ENSAR. We acknowledge support by the Foundation for Polish Science - MPD program, co-financed by the European Union within the European Regional Development Fund.

- 
- [1] *Dynamics and Thermodynamics with nuclear degrees of freedom*, Edited by P. Chomaz, F. Gulminelli, W. Trautmann and S. Yennello (Springer, 2006), Eur. Phys. J. A 30, issue 1, pag. 1–251.
- [2] E. Galichet et al., Phys. Rev. C 79, 064614 (2009).
- [3] D.V. Shetty, S.J. Yennello, and G.A. Souliotis, Phys.

- Rev. C 76, 024606 (2007).
- [4] Bao-An Li, Lie-Wen Chen, and Che Ming Ko, Phys. Rep. 464, 113 (2008).
- [5] M. Di Toro et al., J. Phys. G 37, 083101 (2010).
- [6] F. Rami et al., Phys. Rev. Lett. 84, 1120 (2000).
- [7] I. Lombardo et al., Phys. Rev. C 84, 024613 (2011).

- [8] E. Geraci et al., Nucl. Phys. A 732, 173 (2004).
- [9] G.A. Souliotis et al., Phys. Lett. B 588, 35 (2004).
- [10] M.B. Tsang et al., Phys. Rev. Lett. 92, 062701 (2004).
- [11] M.B. Tsang et al., Phys. Rev. Lett. 102, 122701 (2009).
- [12] Z.Y. Sun et al., Phys. Rev. C 82, 051603(R) (2010).
- [13] M. Veselsky et al., Phys. Rev. C 62, 041605(R) (2000).
- [14] E. De Filippo et al., Phys. Rev. C 86, 014610 (2012).
- [15] A.B. McIntosh et al., Phys. Rev. C 81, 034603 (2010).
- [16] S. Piantelli et al., Phys. Rev. C 74, 034609 (2006).
- [17] V. Baran et al., Phys. Rep. 410, 335 (2005).
- [18] Lie-Wen Chen, Che Ming Ko, and Bao-An Li, Phys. Rev. Lett. 94, 032701 (2005).
- [19] T.X. Liu et al., Phys. Rev. C 76 (2007) 034603
- [20] D. Theriault et al., Phys. Rev. C 74, 051602 (2006).
- [21] R. Lioni et al., Phys. Lett. B 625, 33 (2005).
- [22] P. Napolitani et al., Phys. Rev. C 81, 044619 (2010).
- [23] *Isospin Physics in Heavy-Ion Collisions at Intermediate Energies*, edited by B.A. Li and W.U. Schröder, (Nova Science, New York, 2001).
- [24] G. Souliotis et al., Phys. Rev. C 68, 024605 (2003).
- [25] M. Colonna et al., Nucl. Phys. A 805, 454c (2008).
- [26] Lie-Wen Chen et al., Phys. Rev. C 80, 014322 (2009).
- [27] E. Galichet et al., Phys. Rev. C 79, 064615 (2009).
- [28] see <http://fazia2.in2p3.fr/spip>
- [29] N. Le Neindre et al., Nucl. Instrum. Methods A 701, 145 (2013).
- [30] Fondazione Bruno Kessler, Trento, Italy.
- [31] L. Bardelli et al., Nucl. Instrum. Methods A 602, 501 (2009).
- [32] L. Bardelli et al., Nucl. Instrum. Methods A 605, 353 (2009).
- [33] Amcrys-H, Kharkov, Ukraine.
- [34] L. Bardelli et al., Nucl. Instrum. Methods A 654, 272 (2011).
- [35] S. Carboni et al., Nucl. Instrum. Methods A 664, 251 (2012).
- [36] G. Pasquali et al., Eur. Phys. J. A 48, 158 (2012).
- [37] S. Barlini et al., in press in Nucl. Instrum. Methods A (2013) <http://dx.doi.org/10.1016/j.nima.2012.12.104i>.
- [38] H. Hamrita et al., Nucl. Instrum. Methods A 531, 607 (2004).
- [39] B. Braunn et al., Nucl. Instrum. Methods B 269, 2676 (2011).
- [40] L.C. Northcliffe and R.F. Schilling, Nucl. Data Tables A 7 (1970) 233.
- [41] F. Hubert, R. Bimbot, and H. Gauvin, Atom. Data Nucl. Data Tables 46 (1990) 1.
- [42] E. De Filippo, rapport Dapnia-SphN-95-60 (1995).
- [43] R. Charity et al., Phys. Rev. C 58, 1073 (1998).
- [44] S. Piantelli et al., Phys. Rev. Lett. 88, 052701 (2002).
- [45] V. Baran et al., Nucl. Phys. A 730, 329 (2004).
- [46] G. Casini et al., Phys. Rev. Lett. 71, 2567 (1993).
- [47] A.A. Stefanini et al., Z. Phys. A 351, 167 (1995).
- [48] J. Wilczynski et al., Phys. Rev. C 81, 024605 (2010).
- [49] A. Pagano et al., Nucl. Phys. A 681, 331c (2001).
- [50] E. De Filippo et al., Acta Phys. Pol. 40, 1199 (2009).
- [51] J.R. Huizenga and W.U. Schroder, in *Treatise on Heavy Ion Science*, edited by D.A. Bromley, (Plenum Press, New York, 1984), Vol. 2, p. 115.
- [52] S. Piantelli et al., Phys. Rev. C 78, 064605 (2008).
- [53] R.J. Charity et al., Nucl. Phys. A 483, 371 (1988).
- [54] P. Napolitani et al., Phys. Rev. C 76, 064609 (2007).
- [55] D. Henzlova et al., Phys. Rev. C 78, 044616 (2008).
- [56] R. Lucas et al., Nucl. Phys. A 464, 172 (1987).
- [57] D. Bazin et al., Nucl. Phys. A 515, 349 (1990).
- [58] M. Di Toro, A. Olmi, and R. Roy, Eur. Phys. J. A 30, 65 (2006).
- [59] J. Colin et al., Phys. Rev. C 67, 064603 (2003).